Amphiphilic copolymers of *N*-vinylpyrrolidone with (di)methacrylates as promising carriers for the platinum(IV) complex with antitumor activity*

S. V. Kurmaz,[a]★ N. V. Fadeeva,[a] B. S. Fedorov,[a]† G. I. Kozub,[a] V. A. Kurmaz,[a] V. M. Ignat'ev,[a,b] and N. S. Emel'yanova[a]

[a] *Institute of Problems of Chemical Physics, Russian Academy of Sciences, 1 prosp. Akad. Semenova, 142432 Chernogolovka, Moscow Region, Russian Federation. Fax: +7 (496) 522 3507. E-mail: skurmaz@icp.ac.ru*
[b] *Faculty of Fundamental Physical and Chemical Engineering, M. V. Lomonosov Moscow State University, 1 Leninskie Gory, 119991 Moscow, Russian Federation*

Water-soluble polymer compositions of the lipophilic complex of *cis*-bis[(nitroxyethyl)-isonicotinamide-*N*]-tetrachloroplatinum(IV) with antitumor activity were prepared. The complex was solubilized by amphiphilic copolymers of *N*-vinylpyrrolidone (VP) with (di)methacrylates synthesized by radical copolymerization in toluene in the absence of any inhibitors of polymer chain growth. Aqueous buffer solutions of the nanostructures were studied by dynamic light scattering, and the influence of the concentrations of the complex and copolymer and temperature on the nanoparticle size (hydrodynamic radius) was estimated. The nanostructures based on the VP copolymer with triethylene glycol dimethacrylate are shown to be thermosensitive and decompose when the temperature rises to physiologically significant values. According to the TEM data, the polymer particles are spherical and contain inclusions of the Pt^{IV} complex ~4 nm in size. The polymer compositions were studied using CV, TGA, and DSC methods. The results of IR spectroscopic analysis of the polymer compositions and quantum chemical modeling indicate the formation of the hydrogen bond between the NH groups of the complex and VP copolymer.

Key words: amphiphilic copolymer of *N*-vinylpyrrolidone, dimethacrylate, platinum(IV) complexes, encapsulation, nanostructures, quantum chemical modeling, hydrogen bond.

The enhancement of the therapeutic effect of anticancer drugs and a decrease in their cytotoxic effect on normal cells demand nanocarriers with high biocompatibility and capability of loading drugs and their controlled and target release in the human organism. Both linear polymers, for example, polyethylene glycol, polylactic or polyglycolic acid, and their copolymers, and branched polymers are presently used as carriers. Dendrimers are considered to be ideal as delivery systems due to the three-dimensional globular network, nanometer dimensions, monodispersity, lipophilicity, and capability of easily penetrating into a cell of the human organism.[1—3] However, their preparation is complicated and multistep, and some dendrimers are very toxic for the cells[4] and must be additionally functionalized.

The amphiphilic polymers with diverse architecture were developed as an alternative to dendrimers,[5] and among them hyperbranched polymers play a special role.[6—9] In spite of irregularity and imperfectness of the architecture, they are highly soluble and have a low viscosity of solution, a high density of the functional groups at the periphery of the macromolecule, and the ability to self-organization in solutions.[10,11] Their significance as carriers of biologically active compounds for pharmacological purposes increases,[9] since they provide the prolonged effect of drugs, change their distribution in the organisms, and decrease toxicity.

One of the simplest and most efficient methods for the preparation of branched copolymers from commercially available vinyl monomers was developed at the University of Strathclyde (Glasgow, Scotland) and was named the Strathclyde methodology.[12] The radical copolymerization of such monomers controlled by the chain transfer agent makes it possible to form branching points using polyfunctional monomers. The amphiphilic copolymers with the branched structure reacting to a change in the temperature or pH of the medium were prepared by this method.[13—15] Using this approach, we pioneered in preparing a line of amphiphilic copolymers of *N*-vinylpyrrolidone (VP) with (di)methacrylates of various structures in the presence[16] or in the absence[17] of 1-decanethiol (chain transfer

* Based on the materials of the VIII All-Russian Kargin Conference "Polymers-2020" (November 9—13, 2020, Moscow, Russia).
† Deceased.

Published in Russian in *Izvestiya Akademii Nauk. Seriya Khimicheskaya,* No. 9, pp. 1832—1844, September, 2021.
1066-5285/21/7009-1832

agent). These copolymers have a low cytotoxicity and can penetrate into the cells.

The results of studies showed that the amphiphilic copolymers of VP with triethylene glycol dimethacrylate can be used as platforms for the synthesis of hydrophilic compounds, for instance, *N*,*N*-dimethylbiguanidine hydrochloride (metformin),[18] or for hydrophobic compounds, such as binuclear tetranitrosyl iron complexes[19,20] and platinum(IV) organic complexes.[21,22] The biocompatible polymer compositions of the platinum(IV) aminonitroxyl complex with the anticancer activity against the *HeLa* cells were prepared.[21] As compared to the platinum(II) complexes (cisplatin and others),[23,24] the platinum(IV) complexes are more inert, characterized by moderate toxicity, and efficient against cisplatin-resistant tumors.[24] To control such properties of the platinum complexes as solubility, bioaccessibility, toxicity, prolonged effect, distribution in the organism, duration of circulation in blood, and accumulation in tumor cells and inflammation centers, they are encapsulated into various carriers: liposomes, micelles, dendrimers, and inorganic or other solid particles.[25—27]

The platinum(IV) complexes[28,29] with a high antimetastatic activity and a low total toxicity against experimental melanoma B-16 and lung carcinoma were synthesized using biogenic low-toxicity compounds (nicotinic and isonicotinic acids) as ligands at the Institute of Problems of Chemical Physics (Russian Academy of Sciences).[28] The synthesized organic Pt^{IV} complexes are readily soluble in DMSO and DMF but are poorly soluble in water and ethanol. The introduction of OH groups into the ligands enhances the solubility of the complexes in water. However, the stability of their aqueous solutions was not improved. The encapsulation of *cis*-bis[2-(nitroxyethyl)isonicotinamide-*N*]-tetrachloroplatinum(IV) ($Pt^{IV}L$)[22] in the amphiphilic biocompatible VP copolymers with (di)methacrylates was proposed to enhance solution stability. This complex is known due to its anticancer activity and capability of generating nitrogen monoxide during biotransformation. The biological assays showed[22] that the $Pt^{IV}L$ complex encapsulated in these copolymers possessed cytotoxic activity toward tumor cells A172, and in 48 h of incubation its dose IC_{50} was about 106 μmol L^{-1}, whereas for the starting complex this value was 91 μmol L^{-1}.

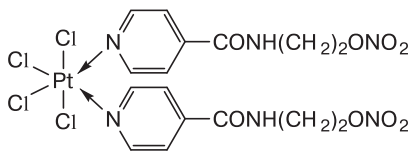

$Pt^{IV}L$

Since the amphiphilic VP copolymers with the branched structure are interesting as carriers and delivery vehicles of $Pt^{IV}L$, the experimental and theoretical study of the corresponding polymer compositions (PC) is an urgent task. The purposes of this work are as follows: preparation of PC of *cis*-bis[2-(nitroxyethyl)isonicotinamide-*N*]-tetrachloroplatinum(IV) on the basis of the amphiphilic VP copolymers with (di)methacrylates, quantum chemical modeling of the structures of the $Pt^{IV}L$—copolymer complexes by the DFT method, and studies of their structures and properties using various physicochemical methods.

Experimental

The *cis*-bis[2-(nitroxyethyl)isonicotinamide-*N*]-tetrachloroplatinum(IV) complex was synthesized from platinum hexachloride potassium salt and *N*-(2-nitroxyethyl)isonicotinamide using an earlier described procedure.[28] The complex was characterized by elemental analyses and IR and NMR spectroscopy.

Isopropyl alcohol (special purity grade, Khimmed, Russia) was used as received. Bidistilled water and a neutral water—salt phosphate buffer (pH 6.8) containing 137 mmol L^{-1} NaCl, 2.68 mmol L^{-1} KCl, 4.29 mmol L^{-1} Na_2HPO_4, and 1.47 mmol L^{-1} KH_2PO_4 (all from Khimmed, Russia) were used. Dimethyl sulfoxide (Lab-Scan, Poland), was purified by freezing out, and the water content in it (⩽0.05%) was monitored by IR spectroscopy using a known procedure.[30]

To prepare copolymers, *N*-vinylpyrrolidone (Alfa Aesar, USA) was purified by distillation *in vacuo* from the NaOH inhibitor. Triethylene glycol dimethacrylate (TEGDM) (Aldrich, USA) and poly(ethylene glycol) methyl ether methacrylate (PEGMEM) (Aldrich) were used as received. The VP—TEGDM and VP—PEGMEM—TEGDM copolymers were prepared at the molar ratio of the monomers 95 : 5 and 95 : 5 : 5, respectively, using radical copolymerization in toluene according to a previously described procedure.[17] The content of the monomers in toluene was about 80%. The azobisisobutyronitrile (AIBN) initiator was 0.01 mol L^{-1}. The copolymers were isolated from solutions by precipitation with a tenfold excess of *n*-hexane (Khimmed, Russia) and dried to a constant weight *in vacuo*. The yield of the copolymers was ~90%. The content of the monomeric units in the copolymers was calculated from the elemental analysis data. Elemental analysis was carried out on a Vario EL cube instrument (Elementar GmbH, Germany). The absolute molecular weights of the copolymers were determined according to a known procedure[17] by exclusion liquid chromatography on a Waters GPCV 2000 instrument (Waters, USA) США) using two detectors: a refractomer (RI) and a light scattering detector (MALLS). The content of platinum in the encapsulated complex was determined by the Pregl chemical analysis, and the chlorine content was determined by mercurimetric titration.[31] Aqueous solutions of PC were studied by the dynamic light scattering (DLS) method at a detection angle of 90° on a Photocor Compact setup (Photocor, USA) at the wavelength 654 nm. Measurements of light scattering by aqueous dispersions were performed after their filtration through a microporous filter (0.45 μm) on a Photocor Compact instrument. Prior to measurements, vials with the solutions were stored at a constant temperature for ~30 min. Experimental data were processed using the DynaLS v. 2.8.3 software. The experimental results of DLS were presented as characteristic times of the correlation functions of scattered light and particle distribution over diffusion coefficients.

The hydrodynamic radius of particles R_h was calculated using the Stokes—Einstein equation: $D = kT/6\pi\eta R$, where k is the Boltzmann constant, T is the absolute temperature, and η is the viscosity of the medium in which dispersed particles are pendant. The absorption spectra of aqueous solutions of $Pt^{IV}L$ and PC were recorded with a SPEKS SSP-705-1 scanning spectrophotometer (Russia) in a quartz cell with a path length of 0.5 cm. The IR spectra of powders of the $Pt^{IV}L$ complex and PC after drying *in vacuo* were detected in the attenuated total reflectance (ATR) mode on a Bruker α FTIR instrument (Bruker, Germany) in the range from 400 to 4000 cm^{-1} (scan number 16). The thermal stability of $Pt^{IV}L$ and related PC was studied by thermal gravimetric analysis (TGA) and differential scanning calorimetry (DSC) on an STA 409C LUXX synchronous thermoanalyzer (NETZSCH, Germany) in argon with a heating rate of 5 deg min^{-1} in the range from 20 to 500 °C (sample weight was 4—6 mg). The visual images of PC were obtained by transmission electron microscopy (TEM) on a Leo 912 AB instrument (Carl Zeiss, Germany). For this purpose, an aqueous solution of PC was introduced into a carrier and dried in air. Cyclic voltammetry (CV) was conducted in an argon atmosphere (working solution volume 10 cm^3) on an IPC-ProL potentiostat (A. N. Frumkin Institute of Physical Chemistry and Electrochemistry, Russian Academy of Sciences) at 25 °C at scan rates ranging from 20 to 1000 mV s^{-1} in aqueous and nonaqueous solutions. A phosphate buffer with an additive of 0.5 mol L^{-1} KCl was used as the supporting electrolyte in aqueous solutions, whereas 0.1 mol L^{-1} tetrabutylammonium hexafluorophosphate was used in nonaqueous solutions (DMSO). A disc glassy carbon (GC) electrode polymerized in the inert PEEK polymer (Als Co., Ltd., Japan) with a surface area of ~2 mm^2 served as the working electrode. The auxiliary electrode was a platinum wire, and the silver chloride reference electrode (Ag/AgCl/KCl) was separated from the working volume of the cell by a porous glass membrane when working in DMSO. All potentials are given *vs* this electrode. Prior to experiment, the GC electrode was polished with a diamond suspension (particle diameter ~1 μm) and then cleaned by the ultrasonic treatment in the medium (water or the corresponding nonaqueous solvent) in which the studies were carried out. The CV experiment was described in detail earlier.[22,30,32] Quantum chemical calculations were performed in terms of the density functional theory (DFT) with the full optimization of the geometry of the starting molecules and their complexes using the Gaussian 09 program.[33] The TPSSh hybrid functional[34] and 6-311++G**//6-31G* basis set were used. Three monomeric units of the copolymer were taken for geometry optimization of the copolymer and obtained products. It was shown[35] taking polyvinylpyrrolidone (PVP) as an example that the region consisting of three monomeric units is sufficient to use for modeling the complexes. The influence of the solvent (water) was taken into account using the polarizable continuum model (PCM). The calculation of frequencies in the optimized geometries of the starting molecules and products showed the absence of imaginary frequency vibrations and, therefore, all optimized structure correspond to potential energy minima.

Preparation of polymer compositions and films. Polymer compositions were prepared from solutions of the VP—TEGDM and VP—PEGMEM—TEGDM copolymers in Pr^iOH and a solution of the $Pt^{IV}L$ complex in DMSO. The concentrations of the reagents, volume ratios of the solutions, and $Pt^{IV}L$ content based on the copolymer are given in Table 1. A solution of $Pt^{IV}L$ in DMSO was added dropwise to bottles with copolymer solutions with permanent magnetic stirring, and then organic solvents were distilled *in vacuo*. A buffer solution (8 mL) with pH 6.8 was added to thus prepared polymer films with various contents of the $Pt^{IV}L$ complex, and the resulting mixtures were heated at 40 °C for 20 min. Transparent solutions (**1**—**4**, **8**, and **9**) or poorly transparent dispersions (**5**—**7** and **10**—**12**) of aqueous buffer solutions of PC were obtained depending on the $Pt^{IV}L$ content and conditions of their formation.

In a blank experiment conducted in the absence of the copolymer, DMSO (0.24 mL) containing $Pt^{IV}L$ (3.1 mg) was

Table 1. Concentrations of the reactants and conditions for PC formation from the copolymers

Polymer composition no.	Concentrations of solutions/mg mL^{-1}		Volume ratio copolymer : $Pt^{IV}L$	$[Pt^{IV}L]$ (%) based on copolymer
	Copolymer	$Pt^{IV}L$		
Composition based on VP—TEGDM				
1	7.2	1.1	4.0 : 0.5	2.0
2	7.2	1.1	4.0 : 1.0	4.0
3	7.2	1.1	4.0 : 2.0	8.0
4	7.2	2.0	4.0 : 1.50	10.7
5*	7.0	12.8	4.0 : 0.24	11.0
6*	3.5	12.8	4.0 : 0.24	22.0
7*	1.0	12.8	4.0 : 0.24	77.0
Composition based on VP—PEGMEM—TEGDM				
8	7.0	2.0	4.0 : 1.50	11.0
9	3.5	12.8	20.00 : 0.12	2.2
10*	7.0	12.8	4.00 : 0.24	11.0
11*	3.5	12.8	4.00 : 0.24	22.0
12*	1.0	12.8	4.00 : 0.24	77.0

* Limited solubility in an aqueous buffer solution.

added to Pr^iOH (4 mL), and opalescence caused, most likely, by a decrease in the solubility of $Pt^{IV}L$ in Pr^iOH was observed. Then organic solvents were distilled, and a dry residue of $Pt^{IV}L$ was dissolved in an aqueous buffer solution (8 mL). An opaque aqueous dispersion was obtained from the complex was precipitated rapidly.

Results and Discussion

Physicochemical characteristics of the copolymers. During the radical copolymerization of TEGDM, one of its double bonds is involved in the main chain growth, and the second bond participates in the formation of side branches, which appears upon the attachment of polymer radicals to its "pendant" C=C bond. Cyclic structures can be formed within the primary chain itself due to intramolecular cyclization. The PEGMEM monomeric units with the bulky substituent (M_n ~500 g mol^{-1}) in the polymer chains create steric hindrances for cyclization and suppress the formation of micro- and macrogels. Under the chosen synthesis conditions, the copolymerization of VP and PEGMEM with the TEGDM bifunctional monomer afford soluble copolymers VP—TEGDM and VP—PEGMEM—TEGDM with side branches.

At the initial stage, the growing radicals of both types predominantly attach TEGDM and PEGMEM due to the high reactivity of the methacrylate monomers.[16] The contribution of VP to the polymerization reaction increases as these monomers are consumed. As a consequence, the three-dimensional structure with the "pendant" double bonds at which the PVP chains are predominantly attached is formed after the polymerization of the active monomers. As a result, the structure is formed in which fragments enriched in methacrylate units and PVP chains can be distinguished.

The average content of the monomer units in the prepared VP copolymers is presented in Table 2. It is seen that they contain units of (di)methacrylates. A decrease in the VP content in the monomer mixture during the synthesis of the ternary copolymer decreases the content of the unit in it. The IR spectra of the copolymers exhibit absorption bands at wavenumbers of 1720 and 1650 cm^{-1} characteristic of the C=O groups of the methacrylate and VP units, respectively. The IR spectrum of the ternary copolymer contains the absorption band at 1100 cm^{-1} corresponding to vibrations of the C—O ether bond in the PEGMEM unit. Owing to the appearance of the PEGMEM units in the polymer chains, the intensity of the absorption bands assigned to stretching vibrations of the CH_2 groups in the 3000—2800 cm^{-1} range increases.

The molecular weight characteristics of the VP copolymers differ noticeably (see Table 2): the values of M_w and polydispersity coefficient (PD) of the ternary VP copolymer are appreciably higher than those for the binary copolymer. Differences in the values of their relative (RI) and absolute (RI+MALLS) molecular weights, as well as a high PD value, indicate a branched nature of their macromolecules.

The amphiphilic VP copolymers consisting of monomeric units of various polarity are soluble in both polar and low-polarity media: chloroform, acetone, and THF. Taking into account the conditions for PC formation, their behavior in polar media, such as Pr^iOH, water, and aqueous buffer solutions, is of special interest. The study of

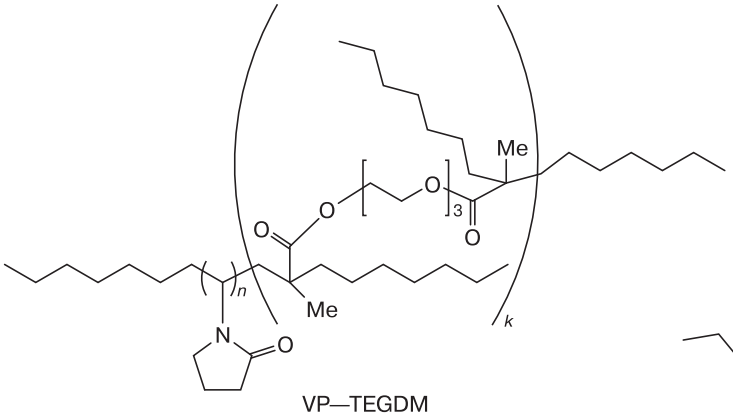

VP—TEGDM

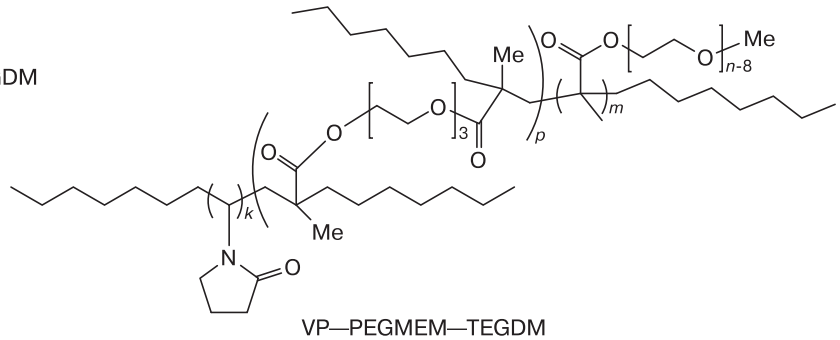

VP—PEGMEM—TEGDM

Table 2. Monomeric composition of the VP copolymers, molecular weights M_w, and polydispersity coefficients (PD)

Copolymer	Molar ratio of units VP : (di)methacrylate (%)	RI		RI+MALLS	
		$M_w \cdot 10^{-4}$	PD	$M_w \cdot 10^{-4}$	PD
VP—TEGDM	90.3 : 9.7	6.4	8.0	8.1	3.2
VP—PEGMEM—TEGDM	89.0 : 11.0	26.0	28.0	35.0	9.2

light scattering by solutions of the VP—TEGDM copolymer in these media by the DLS method[32] show that the size of scattering centers and their size distribution depend on the copolymer concentration. Alcoholic (7 mg mL^{-1}) and aqueous buffer (3.5 mg mL^{-1}) solutions along with small particles (4 nm) contain entities with the hydrodynamic radius R_h equal to 30 and 90 nm, respectively. Their response to a temperature change brings about appreciable opalescence in the aqueous buffer solution already at 40 °C.

Now we can consider the results of the DLS study of the ternary VP copolymer. Based on the dependences of the light scattering intensity I on the ternary copolymer concentration constructed in the semilogarithmic coordinates, we estimated the critical concentrations of aggregation (CAC), which are 0.47 and 0.65 mg mL^{-1} in Pr^iOH and water, respectively. Thus, the PC were obtained at the copolymer concentrations higher than the CAC; *i.e.*, under conditions where the solution contains polymer aggregates.

Figure 1, *a* shows the dependences of the particle size distribution of the light scattering intensity by solutions of the VP—PEGMEM—TEGDM copolymer in Pr^iOH at the concentrations higher and lower than the CAC. The dilute alcoholic solution of the copolymer (0.5 mg mL^{-1}) contains particles of three types with the hydrodynamic radius 3, 36, and $>10^3$ nm. The small particles represent individual macromolecules of the micellar type, since the fragments differed in monomer composition can be distinguished in the macromolecule, and others are their aggregates. The main contribution (about 90%) is made by the particles with a radius of 36 nm. The main peak of the particles of an average size becomes narrower (Fig. 1, *a*) as the copolymer concentration in Pr^iOH increases.

Figure 1, *b* shows the concentration dependences of the distribution of the light scattering intensity by aqueous solutions of the ternary copolymer indicating that the solution contains particles of various dimensions (R_h clustered at ~6 nm) and their aggregates with R_h ~50 nm. It is most likely that an increase in the size of individual macromolecules compared to Pr^iOH solutions is due to the high thermodynamic affinity of water to this copolymer. A comparative analysis of the dependences of the light scattering distribution by aqueous solutions of diverse concentrations showed that the copolymer concentration exerted no effect on the size of the scattering centers in water. However, in an aqueous buffer solution the particle dimensions at the peak maxima are close to those observed in Pr^iOH but lower than those in bidistilled water (Fig. 1, *c*). This means that the macromolecules are weakly swollen in the presence of salts. The study of the temperature effect on the scattering center sizes in a dilute aqueous solution of the copolymer (0.5 mg mL^{-1}) showed that in the range from 30 to 40 °C R_h was ~55 nm. However, with further increasing temperature R_h decreases to 35 nm, probably, due to the destruction of thermosensitive aggregates. Thus, the structures of the polymer solutions, sizes of the aggregates, and their size distribution depend on the com-

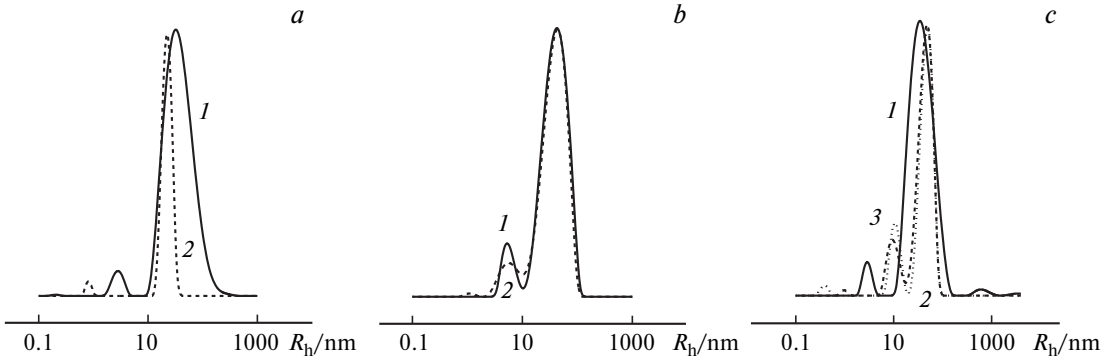

Fig. 1. Effect of the size of scattering centers on the distribution of the light scattering intensity by alcoholic (*a*) and aqueous (*b*) solutions of the ternary copolymer with concentrations of 0.5 (*1*) and 3.5 mg mL^{-1} (*2*) at 25 °C and by an aqueous buffer solution of the ternary copolymer (*c*) (0.5 mg mL^{-1}) at 25 (*1*), 30 (*2*), and 37 °C (*3*).

position of the copolymer, its concentration, and temperature.

Physicochemical properties of the polymer compositions and their behavior in aqueous solutions. It is assumed that the solubilization of $Pt^{IV}L$ by individual macromolecules of the micellar type and their aggregates results in the formation of nanostructures of the host—guest type in which the guest molecules are retained by nonvalent interactions with the functional groups of the copolymer. The solvent Pr^iOH, which like water is thermodynamically unfavorable for the Pt complex, stimulates the formation of complexes between the carrier and active compound. Some PC are completely soluble in an aqueous buffer solution, while other are characterized by limited solubility (see Table 1). Remarkably, compositions **4** and **5** containing the equal amounts of the $Pt^{IV}L$ complex (~11%) had different solubilities in an aqueous buffer solution. This is possibly related to the conditions for the formation of compositions **4** and **5** that imply the use of solutions of $Pt^{IV}L$ in DMSO of various concentrations and their introducion into an alcoholic solution of the copolymer in amounts of 1.50 and 0.24 mL, respectively. It is most likely that the high content of DMSO in a mixture with Pr^iOH results in a change in the structure of a polymer solution in favor of individual macromolecules, their swelling in a Pr^iOH—DMSO mixture, and penetration of molecules of the $Pt^{IV}L$ complex into the internal cavities of the macromolecule. As a result, a high solubility of PC **4** in an aqueous buffer solution is observed. In the case of compositions **8** and **10** containing ~11% $Pt^{IV}L$, there is a similar situation: PC **10** is only partially soluble in an aqueous buffer solution unlike composition **8**. It cannot be excluded that a decrease in the solubility is caused by the localization of $Pt^{IV}L$ in the external shell of a polymer particle and formation of intermolecular complexes due to two substituents: $-CONH(CH_2)_2ONO_2$ in the heterocyclic fragments of $Pt^{IV}L$.

The absorption spectra of aqueous buffer solutions of $Pt^{IV}L$ and PC **1**—**3** are presented in Fig. 2. The absorption at 250—300 nm as a poorly resolved band (shoulder) corresponded to the $Pt^{IV}L$ complex and(or) its encapsulated forms. The absorption band intensity increased with increasing $Pt^{IV}L$ concentration in the solution. The characteristic absorption of the complex in the range about 200 nm was superimposed by the intrinsic absorption of the copolymer. The absorption of $Pt^{IV}L$ was observed in the aqueous buffer solution obtained in the blank experiment, but, unlike solutions of the PC, this solution turned out to be unstable, and the particles of the $Pt^{IV}L$ complex precipitated.

The results of the DLS study of the behavior of aqueous buffer solutions of PC **1**—**3** with various contents of $Pt^{IV}L$ based on the VP—TEGDM copolymer in the wide temperature range from 20 to 50 °C are shown in Fig. 3. It is seen from the temperature dependences of the light

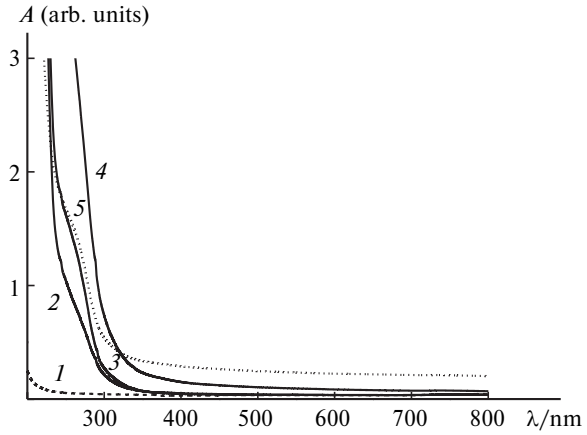

Fig. 2. Absorption spectra of an aqueous buffer solution (*1*); polymer compositions **1** (*2*), **2** (*3*), and **3** (*4*), and complex $Pt^{IV}L$ (*5*); cell thickness 0.5 cm.

scattering intensity by solutions of the corresponding nanostructures **1**—**3** (Fig. 3, *a*) and of the scattering center size (Fig. 3, *b*) that the intensity of light scattering by the solution with a decreased concentration of PC **2** decreases regularly. For solutions of PC **1**—**3** (0.88 mg mL^{-1}), the *I* value decreases with an increase in the $Pt^{IV}L$ content. The shape of the $I(T)$ dependence is determined by the PC concentration: in a concentrated solution of composition **2** the dependence is described by a steeper curve, whereas in a dilute solution the curve becomes flatter. For compositions **1**—**3**, the *I* values increase with temperature. The light scattering intensity by an aqueous solution of PC **2** (3.5 mg mL^{-1}) change jumpwise in a range of 30—37 °C, and its size distribution of the scattering centers becomes unimodal. Scattering centers with R_h ~40 nm appear in a slightly opalescent solution of the composition. The further temperature increase results in an increase in opalescence, but this process is reversible, which is likely caused by a change in the structure of the solution due to the self-organization of the particles reacting to a temperature change. Figure 3, *b* shows that R_h of scattering centers of PC **2** in solutions of various concentrations is nearly the same and does not exceed a value of 40 nm in the studied temperature range. For compositions **1** and **3**, R_h is appreciably higher in the 20—30 °C range but decreases to 40—50 nm with temperature.

An analysis of the light scattering intensity by aqueous buffer solutions of PC **4** with various concentrations is shown in Fig. 4. Figure 4, *a* shows that the light scattering intensity decreases with dilution of the solution and its temperature dependence is described by flatter curves. For the copolymer content in the solution equal to 3.5 mg mL^{-1}, already at 37 °C *I* reaches threshold values of $\sim 2 \cdot 10^6$ cps characteristic of heterogeneous systems. Opalescence is reversible, and the solution again becomes transparent on cooling. In a more dilute solution

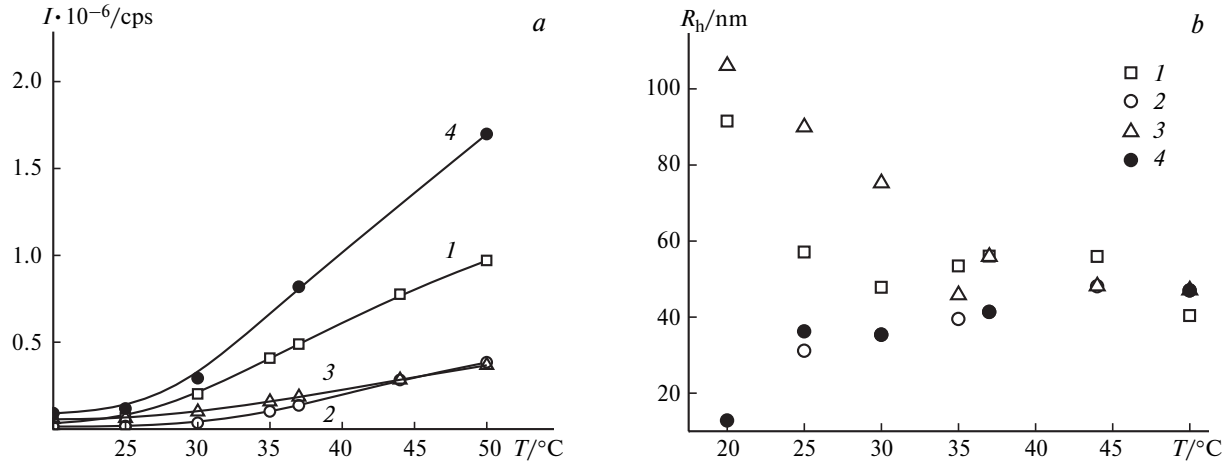

Fig. 3. Intensity of light scattering (*a*) by aqueous buffer solutions of polymer compositions **1** (*1*), **2** (*2*, *4*), and **3** (*3*) and the size of the scattering centers R_h (*b*) as a function of temperature; concentrations of the VP—TEGDM copolymer in the solutions: 0.88 (*1*—*3*) and 3.5 (*4*) mg mL^{-1} for PC **2**.

(1.75 mg mL^{-1}), $I \sim 2 \cdot 10^6$ cps is achieved only at 50 °C. The light scattering intensity by the solution containing 0.88 mg mL^{-1} copolymer does not reach the threshold value even at 60 °C. The light intensity distribution over scattering center sizes is polymodal in all cases, and R_h is temperature-dependent (Fig. 4, *b*). The size increases for the particles of two types in the most concentrated solution (3.5 mg mL^{-1} based on the polymer), which is due to the lowest critical temperature of dissolution of PC **4** at 30—40 °C. In more dilute solutions, the temperature dependence of R_h shows another pattern: the size of the scattering centers decreases with temperature.

The results of the DLS study of aqueous buffer solutions of PC **8** based on the VP—PEGMEM—TEGDM copolymer obtained by the sequential dilution of the solution with a concentration of 3.5 mg mL^{-1} are presented in Fig. 5. It is seen that the light scattering intensity decreases with a decrease in the content of composition **8** in the solution (Fig. 5, *a*). Unlike the PC based on the VP—TEGDM copolymer, the *I* value for PC **8** responses slightly to variations in the studied range. Evidently, this is associated with the presence of the PEGMEM units in the polymer chains shifting the lower critical temperature of dissolution to the range of higher values. The size distribution of the light scattering intensity is also polymodal, but the medium-size particles contribute mainly to the light scattering. The temperature dependences of their hydrodynamic radius are shown in Fig. 5, *b*. It is seen that the size of the scattering centers is higher in the most concentrated solution and decreases with dilution. However, the temperature increase exerts the same effect, which indicates their aggregative nature.

The *I* value is linearly related to the concentration of the scattering centers and, hence, their relative amount in

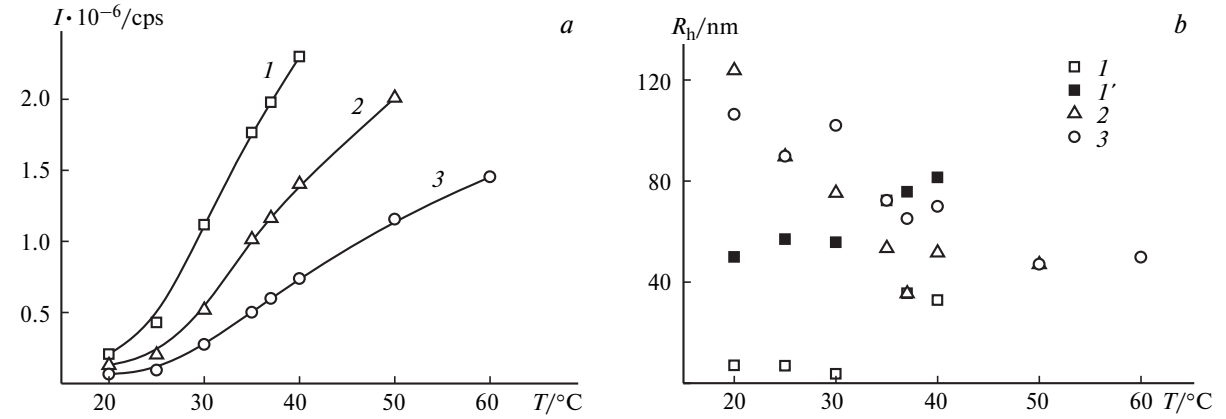

Fig. 4. Intensity of light scattering (*a*) by aqueous buffer solutions of PC **4** ($[Pt^{IV}L]$ = 10.7 wt.%) and hydrodynamic radii R_h of the scattering centers (*b*) as a function of temperature; concentrations of the VP—TEGDM copolymer in the solutions: 3.5 (*1*), 1.75 (*2*), and 0.88 mg mL^{-1} (*3*); *b*: dark (*1′*) and light (*1*) squares designate the R_h values of the scattering centers that make the main contribution to light scattering.

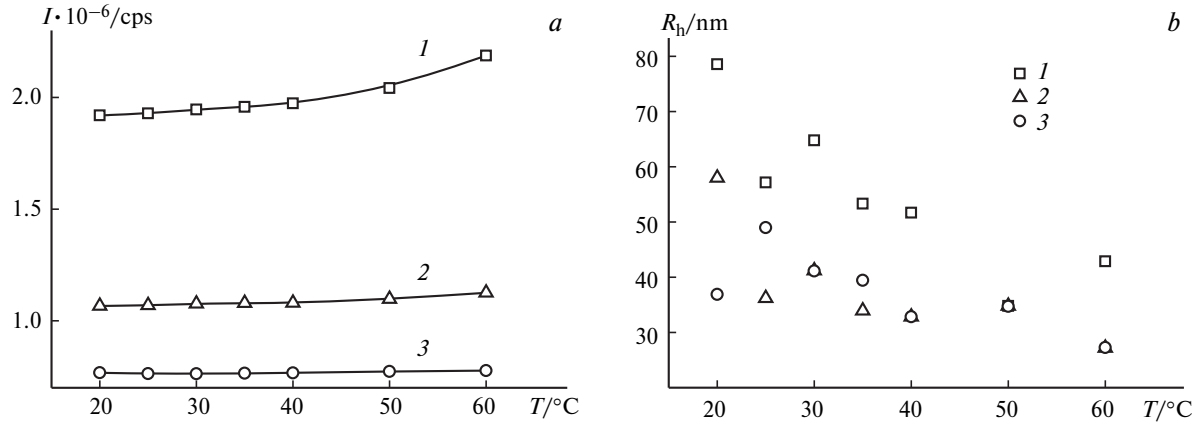

Fig. 5. Intensity of light scattering (*a*) by aqueous buffer solutions of PC **8** ([Pt^{IV}L] = 10.7 wt.%) and the size of the scattering centers (*b*) as a function of temperature; concentrations of the VP—PEGMEM—TEGDM copolymers in the solutions: 3.5 (*1*), 1.6 (*2*), and 0.8 mg mL^{-1} (*3*).

the solutions can be estimated from the light scattering intensity by aqueous buffer solutions containing soluble moieties of PC **10—12**. The contents of PC **11** and **12** decreases compared to that in composition **10** in a solution to reach values of 60 and 20%, respectively. Aqueous solutions of PC **10** and **11** contain mainly aggregates of two types, which appreciably differ in the value of R_h. The sizes of the second type aggregates can be as large as ~70—100 nm, and they respond slightly to temperature variations. In an aqueous solution of the most poorly soluble PC **12**, the size of the aggregates of the second type decreases reaching 50 nm in the temperature range between 36 and 40 °C. However, micronic particles appear that contribute noticeably to the light scattering.

Electrochemical data can be considered as an additional although indirect proof in favor of the fact that the Pt^{IV}L molecule exists in the polar shell as well. Figure 6 presents the CV curves of PC **11** in DMSO and in an aqueous phosphate buffer at various potential sweep rates. It is seen that they differ substantially. The CV curves of free and encapsulated Pt^{IV}L in DMSO are similar in shape (Fig. 6, *a* and *c*). They are complicated in character and contain from 4 to 5 irreversible diffusion waves. Only one broad wave is observed on the CV curves for polymer composition **11** in the potential range where three waves are observed for DMSO solutions, and other waves are absent to −1.6 V (Fig. 6, *b*).

Possibly, a change in the nature of the depolarizer due to hydrogen bond formation can be so strong that its electrochemical behavior in aqueous buffer solutions would be quite different than that in DMSO where Pt^{IV}L molecules are released from the polymer particles. Meanwhile, in other case, the behavior can be similar whether the depolarizer itself occurs in the free form or is encapsulated in the polymer nanoparticles. For example, the CV curves for hydrophobic zinc tetraphenyl porphyrinate in non-aqueous solutions (DMSO, MeCN) and encapsulated in the copolymer of this dye in a neutral aqueous buffer contain its oxidation wave at the Au electrode at close potentials.[32]

The experimental values of Pt (~4%) and Cl (~4%) in composition **5** (11%) are satisfactorily consistent with the calculated values, which indicates the stability of the Pt^{IV}L complex in the course of PC formation. The TEM images

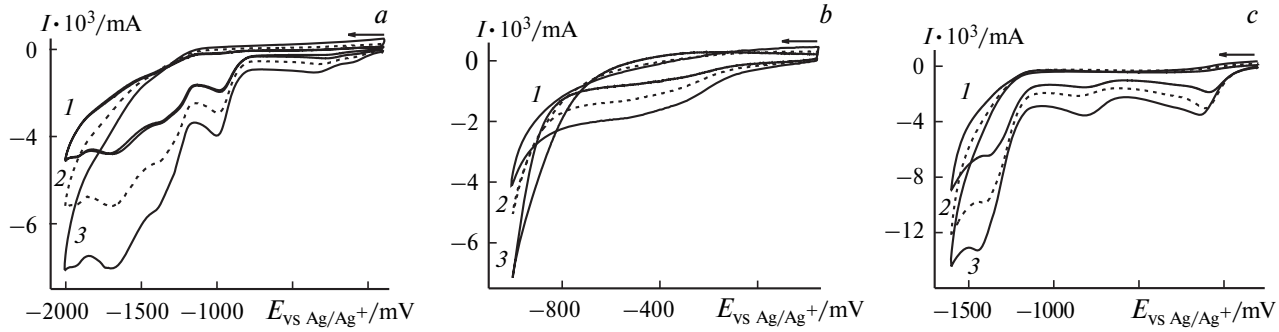

Fig. 6. CV curves at the GC electrode of encapsulated Pt^{IV}L (PC **11**) in DMSO + 0.1 mol L^{-1} $TBAPF_6$ (*a*) and in an aqueous phosphate buffer solution + 0.5 mol L^{-1} KCl (*b*) and of the initial platinum(IV) complex in DMSO + 0.1 mol L^{-1} $TBAPF_6$ (*c*) at the potential sweep rates 20 (*1*), 50 (*2*), and 100 mV s^{-1} (*3*), [Pt^{IV}L] = 1.6 mmol L^{-1} in DMSO.

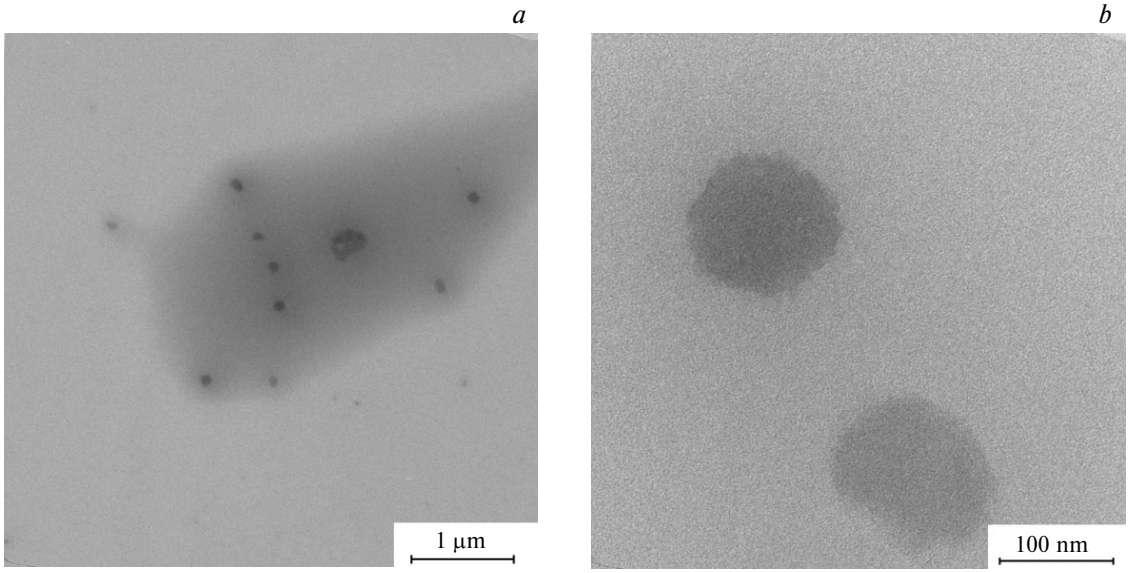

Fig. 7. TEM image of PC **9** based on the VP—PEGMEM—TEGDM copolymer.

of composition **9** in an aqueous solution are shown in Fig. 7. The images demonstrate spherical particles ~130 nm in diameter in which small inclusions (~4 nm) can be distinguished, which represent, most likely, aggregates of $Pt^{IV}L$ molecules.

Moreover, the starting complex retains stability at a temperature of 100 °C and undergoes multistep decomposition at higher temperatures (Fig. 8, *a*). The corresponding exothermic peaks are observed on the DSC curve (Fig. 8, *b*). According to published data,[28] the melting point of the platinum(IV) complex is ~200 °C, and the melting process is accompanied by decomposition. Owing to a low content in PC **9**, the $Pt^{IV}L$ complex exerts almost no effect on the thermal stability of the copolymer and controlled heat release.

Powders of PC **5**—**7** and **11** were studied by IR spectroscopy (Fig. 9). The IR spectra of the copolymers and $Pt^{IV}L$ complex, which is characterized by strong and moderate absorption bands of the organic ligands (ν/cm^{-1}: 3342, 1703, 1650, 1613, 1546, 1495, 1425, 1364, 1274, 1227, 1164, 1114, 1070, 1012, 896, 851, 763, 712, 692, 626, 566, 531, and 459), are presented for comparison. The IR spectra of the PC contain the absorption bands of the copolymers: the strongest bands in a range of 1800—1500 cm^{-1} are attributed to stretching vibrations of the C=O group in the VP and methacrylate units. The IR spectra of the copolymers exhibit a broad absorption band at 3400 cm^{-1} characteristic of stretching vibrations of the OH groups bound by the hydrogen bond to the C=O groups of the lactam cycle.[18] No substantial changes in the structures of the copolymers containing the $Pt^{IV}L$ complex are observed. However, the absorptions in the range of stretching vibrations of OH groups change with an increase in the concentration of the $Pt^{IV}L$ complex for

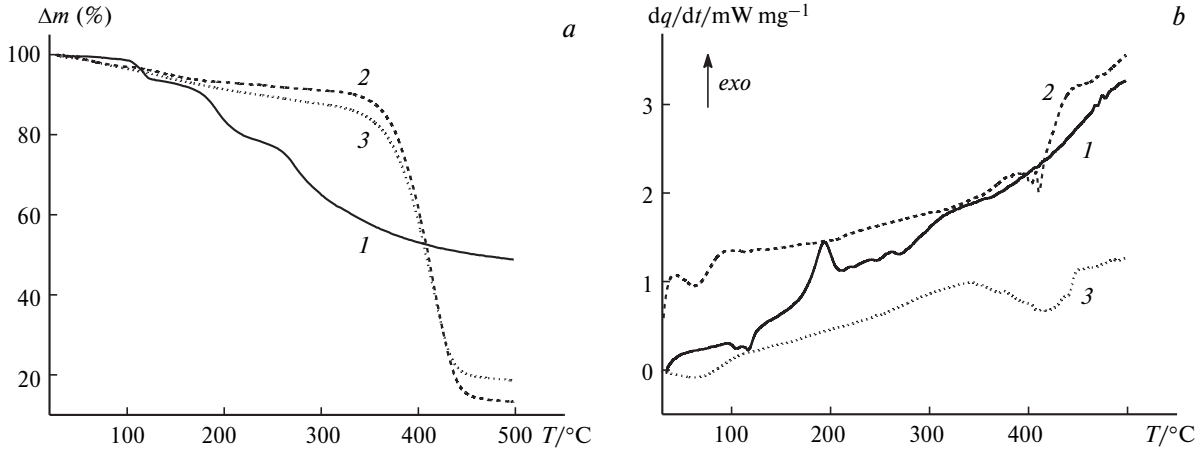

Fig. 8. TGA (*a*) and DSC (*b*) curves for $Pt^{IV}L$ (*1*), ternary copolymer VP—PEGMEM—TEGDM (*2*), and PC **9** (*3*).

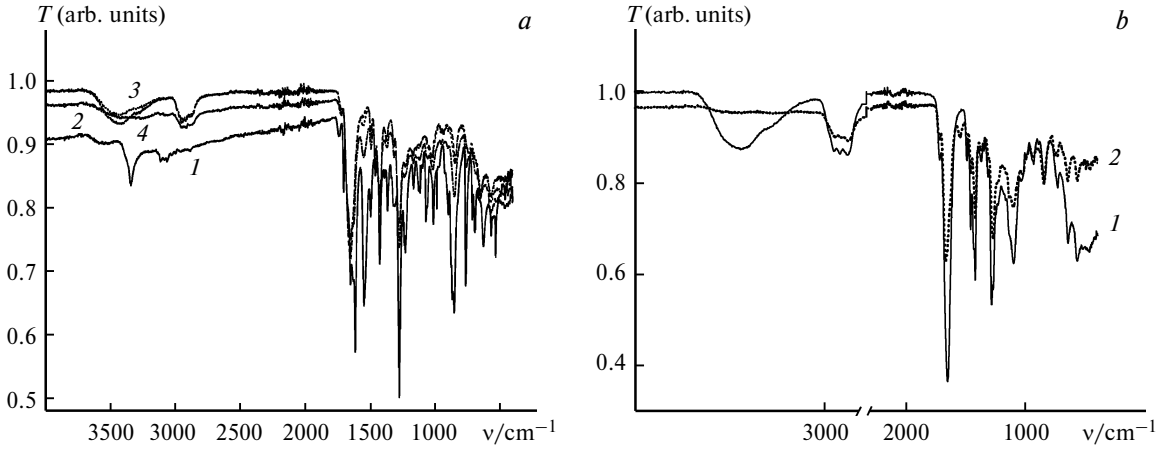

Fig. 9. IR spectra of complex $Pt^{IV}L$ (*1*) and compositions **5**—**7** (*2*—*4*, respectively) (*a*) and copolymer VP—PEGMEM—TEGDM (*1*) and PC **11** (*2*) (*b*).

both VP—TEGDM (Fig. 9, *a*) and VP—PEGMEM—TEGDM (Fig. 9, *b*) copolymers. Moreover, the absorption band assigned to stretching vibrations of the NH group of the $Pt^{IV}L$ complex is nearly absent in the IR spectra detected for the samples with the high PC content. This can be caused by the formation of a hydrogen bond between this group and C=O groups of VP of the lactam cycle of the units. This process can be accompanied by the displacement of water molecules from the hydrate shell of the copolymers.

Quantum chemical modeling of the structures of the $Pt^{IV}L$—copolymer complexes. The quantum chemical modeling of the structures of complexes $Pt^{IV}L$—fragment of the copolymer region consisting of three monomeric units was performed to study the nature of hydrogen bonds in more detail. The oxygen atoms of the lactam cycle act as hydrogen bond acceptors in the formation of hydrogen bonds between the VP—VP—VP region and $Pt^{IV}L$ (Fig. 10, structures pta1 and pta3).

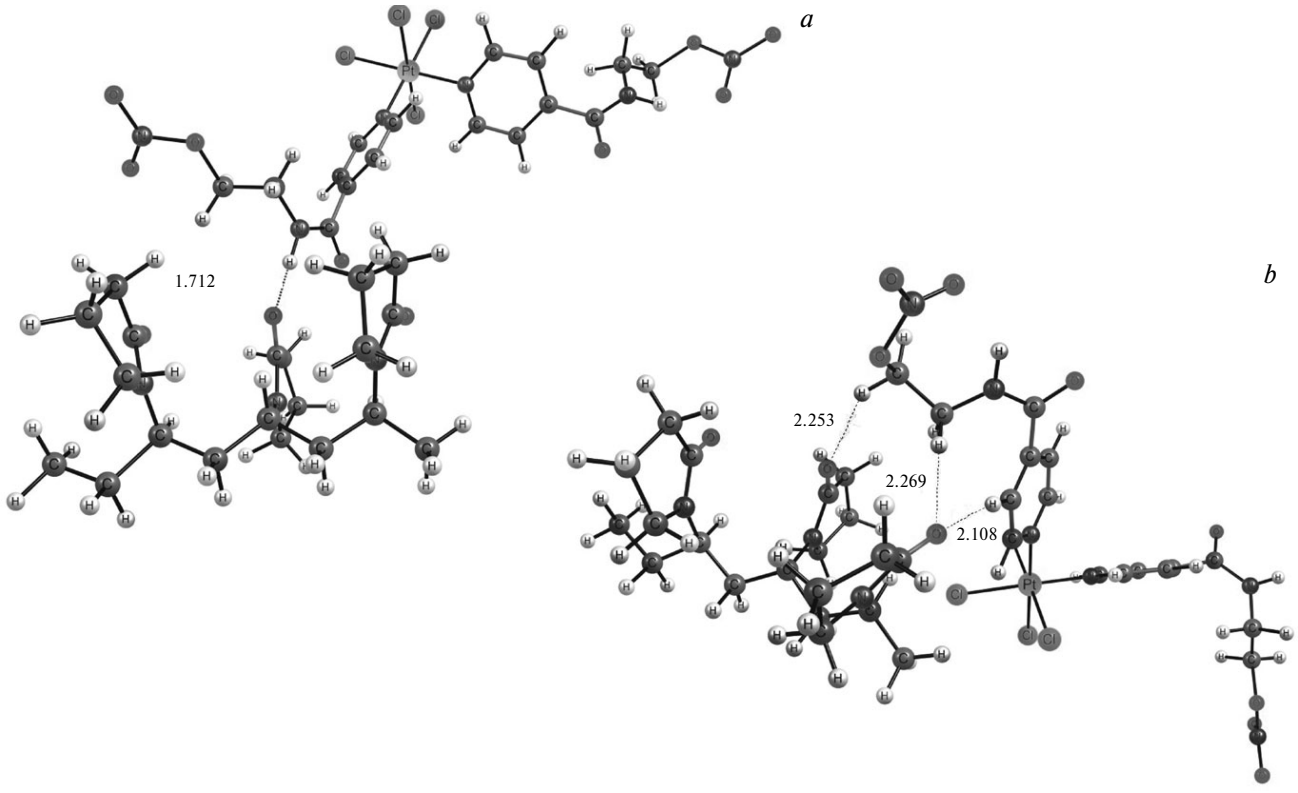

Fig. 10. Structures of complexes pta1 (*a*) and pta3 (*b*).

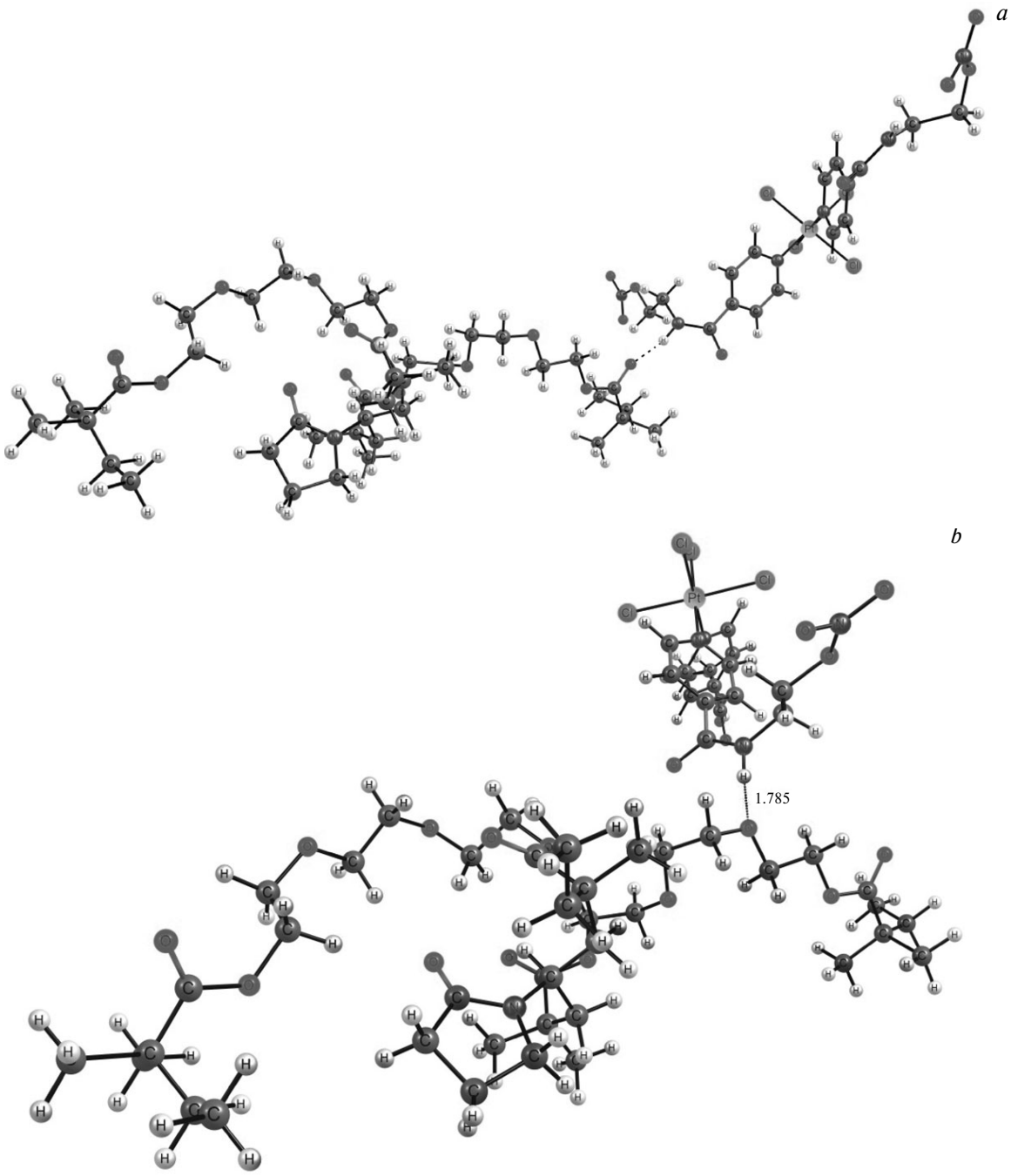

Fig. 11. Structures of complexes ptb2 (*a*) and ptb3 (*b*).

In addition to the carbonyl oxygen atom of the lactam cycle, the oxygen atoms in the TEGDM units (Fig. 11, structures ptb2 and ptb3) can be hydrogen bond acceptors.

Since the $Pt^{IV}L$ complex contains the C=O and NO_2 groups bearing lone electron pairs, hydrogen bonds can be formed for which the copolymers are donors of hydrogen bonds due to the hydrogen atoms in the alkyl groups. However, they are so weak (the energy of hydrogen bonds is lower than 1 kcal mol^{-1}) that their contribution is insignificant.

According to the calculations, the $Pt^{IV}L$ complex forms hydrogen bonds primarily due to the hydrogen atom of the amide group (pta1, ptb2, and ptb3), but the structure can exist in which the hydrogen atoms of the alkyl groups (pta3) are donors of the hydrogen bond.

The values of electron density (ρ) and Laplacian of electron density ($^2\rho$) varying within 0.002—0.040 and 0.024—0.139 a.u., respectively, could be used as evidence for the presence of a hydrogen bond.[36] The most part of the considered bonds fall on this range with the ex-

Table 3. Parameters of hydrogen bonds in the structures of the $Pt^{IV}L$—copolymer compositions

Structures	ρ/a.u.	^{2}ρ/a.u.	E_{bond}/kcal mol^{-1}
pta1	+0.044452	+0.157642	−13.3
pta3	+0.016093	+0.079179	−4.2
	+0.013652	+0.059365	−3.0
	+0.012939	+0.055573	−2.9
ptb2	+0.031589	+0.134589	−9.6
ptb3	+0.038302	+0.138709	−11.2

ception for the bonds in the pta1 and pta3 complexes (Table 3).

The bond formed in the pta1 complex has higher values of ρ and $\nabla^2\rho$, indicating its partially covalent character. The bonds formed in the pta3 complex have lower ρ and $\nabla^2\rho$ values, which can indicate a higher contribution of the van der Waals interactions to this type of binding. The bond energy (E_{bond}) decreases along with the ρ and $\nabla^2\rho$ values, but their cooperative character merits consideration. The total bond energy in the pta3 complex is −10.1 kcal mol^{-1}, which suggests the binding of the platinum(IV) complex with the VP copolymers by the hydrogen atoms in the alkyl groups.

Thus, the water-soluble compositions of *cis*-bis[(nitroxyethyl)isonicotinamide-*N*]-tetrachloroplatinum(IV) with a high content of the active substance (~11%) were prepared from the amphiphilic copolymers of VP. As in the case of PC with a low content of the $Pt^{IV}L$ complex (2%),[22] the cytotoxic effect can be expected when total concentrations of PC and, accordingly, those of the polymer-carrier are reduced. In this way its side toxicity for the human organism can be decreased. It is assumed that the cytotoxic effect against cancer cells of the encapsulated $Pt^{IV}L$ complex can be observed due to its release from the polymer particles, intracellular biotransformation, reduction to platinum(II),[37] and formation of DNA—platinum adducts.[38] Possibly, a lower dose of the active substance would be required for the target delivery of the $Pt^{IV}L$ complex using the modern polymer-carriers to achieve an effect, which would allow one to diminish its toxic effect *in vivo*.

The authors are grateful to E. O. Perepelitsyna for chromatographic analysis of the copolymers and to R. A. Manzhos for help in CV experiment and useful discussion.

This work carried out in the framework of state assignment (Themes Nos. AAAA-A19-119041090087-4, AAAA-A19-119032690060-9, AAAA-A19-119071890015-6, and AAAA-A19-119061890019-5) using equipment of the Analytical Center for Collective Use at the Institute of Problems of Chemical Physics (Russian Academy of Sciences).

This paper does not contain descriptions of studies on animals or humans.

The authors declare no competing interests.

References

1. A. K. Mandal, *Int. J. Polym. Mater. Polym. Biomater.*, 2020, **70**, 287; DOI: 10.1080/00914037. 2020.1713780.
2. M. Kalomiraki, K. Thermos, N. A. Chaniotakis, *Int. J. Nanomed.*, 2016, **11**, 1; DOI: 10.2147/IJN.S93069.
3. R. M. Kannan, E. Nance, S. Kannan, D. A. Tomalia, *J. Int. Med.*, 2014, **276**, 579; DOI: 10.1111/joim.12280.
4. A. Agrawal, S. Kulkarni, *Int. J. Res. Dev. Pharm. Life Sci.*, 2015, **4**, 1700.
5. I. V. Ivanov, T. K. Meleshko, A. V. Kashina, A. V. Iakimanskii, *Russ. Chem. Rev.*, 2019, **88**, 1248; DOI: 10.1070/RCR4870.
6. C. Gao, D. Yan, *Progr. Polym. Sci.*, 2004, **29**, 183; DOI: 10.1016/j.progpolymsci.2003.12.002.
7. N. M. B. Smeets, *Eur. Polym. J.*, 2013, **49**, 2528; DOI: 10.1016/j.eurpolymj.2013.05.006.
8. C. M. Paleos, D. Tsiourvas, Z. Sideratou, L.-A. Tziveleka, *Exp. Opin. Drug Deliv.*, 2010, **7**, 1387; DOI: 10.1517/17425247.2010.534981.
9. X. Zeng, Y. Zhang, Z. Wu, P. Lundberg, M. Malkoch, A. M. Nyström, *J. Polym. Sci. Part A: Polym. Chem.*, 2011, **50**, 280; DOI: 10.1002/pola.25027.
10. Y. Zhou, D. Yan, *Chem. Commun.*, 2009, **9**, 1172; DOI: 10.1039/B814560C.
11. Y. Zhou, W. Huang, J. Liu, X. Zhu, D. Yan, *Adv. Mater.*, 2010, **22**, 4567; DOI: 10.1002/adma.201000369.
12. N. O´Brien, A. McKee, D. C. Sherrington, A. T. Slark, A. Titterton, *Polymer*, 2000, **41**, 6027; DOI: 10.1016/S0032-3861(00)00016-1.
13. M. Luzon, C. Boyer, C. Peinado, T. Corrales, M. Whittaker, L. Tao, T. P. Davis, *J. Polym. Sci., Part A: Polym. Chem.*, 2010, **48**, 2783; DOI: 10.1002/pola.24027.
14. P. Chambon, L. Chen, S. Furzeland, D. Atkins, J. V. M. Weaver, D. J. Adams, *Polym. Chem.*, 2011, **2**, 941; DOI: 10.1039/C0PY00369G.
15. P. Besenius, S. Slavin, F. Vilela, D. C. Sherrington, *React. Funct. Polym.*, 2008, **68**, 1524; DOI: 10.1016/j.reactfunctpolym.2008.08.004.
16. S. V. Kurmaz, A. N. Pyryaev, *Polymer Sci., Ser. B*, 2010, **52**, 1; DOI:10.1134/S156009041001001X.
17. S. V. Kurmaz, N. A. Obraztsova, A. A. Balakina, A. A. Terent´ev, *Russ. Chem. Bull.* (*Int. Ed.*), 2016, **65**, 2097; DOI: 10.1007/s11172-016-1558-x.
18. S. V. Kurmaz, N. V. Fadeeva, V. M. Ignat´ev, V. A. Kurmaz, S. A. Kurochkin, N. S. Emel´yanova, *Molecules*, 2020, **25**, 6015; DOI: 10.3390/molecules25246015.
19. S. V. Kurmaz, T. N. Rudneva, N. A. Sanina, *Mendeleev Commun.*, 2018, **28**, 73; DOI: 10.1016/j.mencom.2018.01.024.
20. T. N. Rudneva, N. S. Emel´yanova, S. V. Kurmaz, *Chem. Papers*, 2019, **73**, 95; DOI: 10.1007/s11696-018-0569-5.
21. S. V. Kurmaz, V. D. Sen, A. V. Kulikov, D. V. Konev, V. A. Kurmaz, A. A. Balakina, A. A. Terent´ev, *Russ. Chem. Bull.*, 2019, **68**, 1769; DOI: 10.1007/s11172-019-2623-z.
22. S. V. Kurmaz, N. V. Fadeeva, B. S. Fedorov, G. I. Kozub, N. S. Emel´yanova, V. A. Kurmaz, R. A. Manzhos, A. A.

Balakina, A. A. Terentyev, *Mendeleev Commun.*, 2020, **30**, 22; DOI: 10.1016/j.mencom.2020.01.007.
23. N. J. Wheate, S. Walker, G. E. Craig, R. Oun, *Dalton Trans.*, 2010, **39**, 8113; DOI: 10.1039/C0DT00292E.
24. S. Dilruba, G. V. Kalayda, *Cancer Chemotherapy and Pharmacology*, 2016, **77**, 1103; DOI: 10.1007/s00280-016-2976-z.
25. V. P. Torchilin, *J. Control. Release*, 2001, **73**, 137; DOI: 10.1016/s0168-3659(01)00299-1.
26. R. Duncan, *Nat. Rev. Drug Discov.*, 2003, **2**, 347; DOI: 10.1038/nrd1088.
27. D. Peer, J. M. Karp, S. Hong, O. C. Farokhzad, R. Margalit, R. Langer, *Nat. Nanotechnol.*, 2007, **2**, 751; DOI: 10.1038/nnano.2007.387.
28. B. S. Fedorov, M. A. Fadeev, G. I. Kozub, S. M. Aldoshin, Z. G. Aliev, L. O. Atovmyan, N. P. Konovalova, T. E. Sashenkova, T. A. Kondrat´eva, S. V. Blokhina, *Pharm. Chem. J.*, 2009, **43**, 134; DOI: 10.1007/s11094-009-0256-5.
29. B. S. Fedorov, M. A. Fadeev, G. I. Kozub, A. N. Chekhlov, N. P. Konovalova, T. E. Sashenkova, E. I. Berseneva, O. V. Dobrokhotova, L. V. Tatyanenko, *Russ. Chem. Bull.*, 2011, **60**, 1181; DOI: 10.1007/s11172-011-0186-8.
30. A. G. Krivenko, A. S. Kotkin, V. A. Kurmaz, *Russ. J. Electrochem.*, 2005, **41**, 137; DOI: 10.1007/s11175-005-0025-z.
31. V. P. Fadeeva, V. D. Tikhova, *Kolichestvennyi elementnyi analiz organicheskikh veshchestv i materialov* [*Quantitative Elemental Analysis of Organic Substances and Materials*], Novosibirsk Gos. Univ., Novosibirsk, 2013, 38 pp. (in Russian).
32. S. V. Kurmaz, V. Yu. Gak, V. A. Kurmaz, D. V. Konev, *Russ. J. Phys. Chem. A*, 2018, **92**, 329; DOI: 10.1134/S0036024418020152.
33. M. J. Frisch, G. Trucks, H. B. Schlegel, G. E. Scuseria, M. A. Robb, J. R. Cheeseman, G. Scalmani, V. Barone, B. Mennucci, G. A. Petersson, H. Nakatsuji, M. Caricato, X. Li, H. P. Hratchian, A. F. Izmaylov, J. Bloino, G. Zheng, J. L. Sonnenberg, M. Hada, M. Ehara, K. Toyota, R. Fukuda, J. Hasegawa, M. Ishida, T. Nakajima, Y. Honda, O. Kitao, H. Nakai, T. Vreven, J. A. Montgomery, J. E. Peralta, F. Ogliaro, M. Bearpark, J. J. Heyd, E. Brothers, K. N. Kudin, V. N. Staroverov, R. Kobayashi, J. Normand, K. Raghavachari, A. Rendell, J. C. Burant, S. S. Iyengar, J. Tomasi, M. Cossi, N. Rega, J. M. Millam, M. Klene, J. E. Knox, J. B. Cross, V. Bakken, C. Adamo, J. Jaramillo, R. Gomperts, R. E. Stratmann, O. Yazyev, A. J. Austin, R. Cammi, C. Pomelli, J. W. Ochterski, R. Martin, L. K. Morokuma, V. G. Zakrzewski, G. A. Voth, P. Salvador, J. J. Dannenberg, S. Dapprich, A. D. Daniels, Farkas, J. B. Foresman, J. V. Ortiz, J. Cioslowski, D. J. Fox, *Gaussian 09*, *Revis. B.01*, Gaussian, Inc., Wallingford CT, 2009.
34. J. Tao, J. P. Perdew, V. N. Staroverov, G. E. Scuseria, *Phys. Rev. Lett.*, 2003, **91**, 146401; DOI: 10.1103/PhysRevLett.91.146401.
35. V. M. Ignat´ev, N. S. Emel´yanova, N. A. Sanina, *Russ. Chem. Bull.*, 2020, **69**, 2265; DOI: 10.1007/s11172-020-3045-7.
36. U. Koch, P. L. A. Popelie, *J. Phys. Chem.*, 1995, **99**, 9747; DOI: 10.1021/j100024a016.
37. M. C. McCormick, K. Keijzer, A. Polavarapu, F. A. Schultz, M.-H. Baik, *J. Am. Chem. Soc.*, 2014, **136**, 8992; DOI: 10.1021/ja5029765.
38. J. J. Wilson, S. J. Lippard, *Inorg. Chem.*, 2011, **50**, 3103; DOI: 10.1021/ic2000816.

Received January 29, 2021;
in revised form June 4, 2021;
accepted June 21, 2021